in practice, may be caused by a person walking near the seismograph pier, or an automobile parked fifty feet away.

Several solutions of this problem of the inertial seismograph come to mind. The first is to design the seismometer transducer for a large linear range. A second is to devise some servo system with a very long time constant for releveling the seismometer frame. A third is to shorten the seismometer period and use of long-period galvanometer to cover the desired pass band—the "inverted" system described earlier in this article.

In addition to the solutions above, and especially for waves having periods of several minutes and above, the seismologist has an entirely different tool at his disposal. This is the horizontal earth strain seismograph, essentially a device which measures the change of distance between two nearby points on the earth's surface as a wave passes by. From the earth strain, so measured, and by knowledge of the specific wave mode, horizontal motions may be deduced. However, discussion of this device, its logical design and installation, should be the subject of a separate paper.

ACKNOWLEDGMENT

In closing, the authors would like to express particular appreciation to H. Matheson of the National Bureau of Standards staff and to J. Hamilton of The Geotechnical Corporation, Garland, Tex.—the former for meticulous checking of numerous statements for clarity, the latter for comments relating to mechanical design experience and for assistance in providing special drawings and photographs of the instruments mentioned. Special thanks are also to be rendered to the editorial "nitpickers" on the NBS staff, without whose assistance this article would probably contain at least several points of confusion.

Investigation of Large-Scale Inhomogeneities in the Earth by the Magnetotelluric Method*

F. X. BOSTICK, JR.†, MEMBER, IRE, AND H. W. SMITH†, SENIOR MEMBER, IRE

Summary—**In the magnetotelluric analysis proposed by Cagniard, a resistivity profile of a homogeneous stratified earth model is determined from the ratio of the tangential components of the natural electric and magnetic fields at the surface of the earth. This type of analysis is often confused by the fact that apparent resistivity estimates obtained from data recorded at one site on different occasions may vary considerably. Also the apparent resistivities computed from one component of the E field and its orthogonal H field component may be significantly different from those computed from another pair of orthogonal field components. Cantwell points out that these variations may, at least in part, be due to two-dimensional inhomogeneities and/or anisotropies together with randomly polarized magnetotelluric fields. Accordingly he has suggested testing the wave impedance of the earth as a rank two tensor.**

This paper describes a measurement and analysis procedure developed using a model based on a two-dimensional wave impedance tensor. It was found that a rotation of the measuring axis to minimize the main diagonal terms in the impedance tensor yields a reasonably consistent estimate of the direction and magnitude of a major inhomogeneity in the apparent resistivity profile.

* Received August 22, 1962. This work was supported by the Office of Naval Research under Contract No. 375(14).

† Electrical Engineering Research Laboratory, University of Texas, Austin, Tex.

INTRODUCTION

IN THE CONVENTIONAL magnetotelluric analysis as developed by Cagniard[1,2] an apparent resistivity, ρ, a scalar function of frequency, is computed from experimental data obtained from simultaneous measurements of the fluctuations of the earth's geomagnetic. and telluric fields. This apparent resistivity function is then compared with similar functions computed for two-dimensionally homogeneous and isotropic stratified earth models. If a similarity between the empirical curve and the curve for a particular model is noted, one concludes that the particular stratified earth model is, at least in a gross sense, representative of the real earth.

For the simple case of a plane wave incident upon a uniform earth the impedance normal to the earth is

[1] Louis Cagniard, "Basic theory of the magnetotelluric method of geophysical prospecting," *Geophysics*, vol. 18, pp. 605–635; 1953.

[2] Louis Cagniard, "Électricité Tellurique," in "Handbuch der Physik," vol. 47, pp. 407–469; 1956.

defined as the ratio of tangential electric and magnetic field intensities. This relation may be expressed

$$E_x/H_y = (\rho\mu\omega)^{1/2}e^{i\pi/4} \tag{1}$$

where ρ is the resistivity in ohm meters, μ is the permeability in henrys/m, ω is the radian frequency, E_x and H_y are orthogonal components of the electric and magnetic fields relative to a reference axis. In addition Cagniard extended the analysis to include the two-layer case, for which he published his master curves.[1]

Several investigators[3,4,5,6,7] have arrived at interpretations for the resistivity of the earth by the application of measured magnetotelluric values to the two-layer Cagniard curves. The frequencies involved have generally been limited to the range from 0.001 to 1 cps. Unfortunately so little is known relative to the resistivity structure of the earth to the depths in question (a hundred kilometers or more at the lower frequencies) that there remains a great deal of uncertainty as to the validity of these interpretations.

It is important to note that the Cagniard model requires resistivity values which are invariant with the orientation of the measuring axis. However, in the results to be presented in this paper a wide variation in the measured values was found as the measuring axis was rotated. Moreover, the measured results were found to vary considerably with data samples taken at the same location on different days. For these reasons it was felt that a more complex model would be required to explain the observed variations. Whether or not these variations are peculiar to the specific location has not been established.

One of the more extensive discussions of increasingly complex earth models is given by Cantwell[5] in his Ph.D. dissertation, in which he outlines procedures for determining the effects of anisotropic and/or two-dimensionally inhomogeneous structures in the earth. In view of the difficulties experienced in obtaining the consistent and repeatable resistivity values required by the Cagniard model, the authors decided to adopt a more complex model following the suggested procedures of Cantwell. In the course of the investigation it was found that certain modifications and extensions of the method were required. It is the subject of this paper to discuss the analysis techniques involved and the results obtained from their application to experimental data.

Theory

As suggested by Cantwell it is assumed that the spectral components of the fluctuations of the tangential electric and magnetic fields at the earth's surface are related by

$$H_i = Y_{ij}E_j; \qquad i, j = 1, 2 \tag{2}$$

where (2) is written in tensor notation. The tangential electric field is given by

$$\bar{E} = \bar{u}_j E_j,$$

and the tangential magnetic field by

$$\bar{H} = \bar{u}_i H_i.$$

The unit vectors $\bar{u}_i$ define an orthogonal coordinate system that is coplanar with and oriented at some angle θ with respect to a reference orthogonal coordinate system defined by the unit vectors $\bar{a}_i$. The quantities Y_{ij}, E_j, and H_i are all functions of radian angular frequency and the orientation angle θ. Both E_j and H_i may be obtained from the time variations of the tangential components of the electric and magnetic fields as the complex Fourier transforms

$$\begin{pmatrix} E_j \\ H_i \end{pmatrix} = \frac{1}{T}\int_{-T/2}^{T/2} \begin{pmatrix} e_j(t) \\ h_i(t) \end{pmatrix} e^{-i\omega t}dt.$$

It is also assumed that for some $\theta=\theta_0$ (2) reduces to

$$\begin{aligned} H_1(\theta_0) &= Y_{12}(\theta_0)E_2(\theta_0) \\ H_2(\theta_0) &= Y_{21}(\theta_0)E_1(\theta_0), \end{aligned} \tag{3}$$

indicating that

$$Y_{11}(\theta_0) = Y_{22}(\theta_0) = 0.$$

Having the orientation θ_0, the unit vectors $\bar{u}_i$, define two axes which are the principal axes of the admittance tensor Y_{ij}. The values of the admittance tensor elements computed for orientations of the unit vectors $\bar{u}_i$ other than $\theta=\theta_0$ may now be expressed in terms of their values along the principal axes and the relative orientation angle $\theta-\theta_0$. Subjecting (3) to a coordinate rotation yields

$$H_i(\theta) = Y_{ij}(\theta - \theta_0)E_j(\theta_0), \tag{4}$$

where

$$\begin{aligned} Y_{11}(\theta-\theta_0) &= [Y_{12}(\theta_0) + Y_{21}(\theta_0)] \sin(\theta-\theta_0)\cos(\theta-\theta_0) \\ Y_{12}(\theta-\theta_0) &= -Y_{21}(\theta_0)\cos^2(\theta-\theta_0) - Y_{12}(\theta_0)\sin^2(\theta-\theta_0) \\ Y_{21}(\theta-\theta_0) &= Y_{21}(\theta_0)\cos^2(\theta-\theta_0) - Y_{12}(\theta_0)\sin^2(\theta-\theta_0) \\ Y_{22}(\theta-\theta_0) &= -[Y_{12}(\theta)_0 + Y_{21}(\theta_0)]\sin(\theta-\theta_0)\cos(\theta-\theta_0). \end{aligned}$$

Eq. (4) has the form of (2) and is consistent with our original assumption.

Cantwell has considered the problem of a plane wave incident on a semi-infinite earth. If the earth consists

[3] T. F. Webster, "An Experimental Investigation of Telluric and Magnetotelluric Phenomena," M.S. thesis, University of Alberta, Edmonton, Canada; 1957.
[4] E. R. Niblett and C. Sayn-Wittgenstein, "Variation of electrical conductivity with depth by the magnetotelluric method," *Geophysics*, vol. 25, pp. 998–1008; October, 1960.
[5] T. Cantwell, "Detection and Analysis of Low Frequency Magnetotelluric Signals," Ph.D. dissertation, M.I.T., Cambridge, Mass.; 1960.
[6] T. Cantwell and T. R. Madden, "Preliminary Report on Crustal Magnetotelluric Measurements," *J. Geophys. Res.*, vol. 65, pp. 4202–4205; December, 1960.
[7] F. X. Bostick, Jr. and H. W. Smith, "An Analysis of the Magnetotelluric Method for Determining Subsurface Resistivities," Elec. Engrg. Res. Lab., University of Texas, Austin, Rept. No. 120; 1961.

of conductive material which is homogeneous but anisotropic in planes lying parallel to the surface, then the principal axes of the computed admittance tensor will coincide with the major axes of the anisotropy. Also considered by Cantwell was the case of a two-dimensionally inhomogeneous but isotropic earth. An example of such a model would be a vertical contact between two media of different conductivity. Here the principal axes of the admittance tensor coincide with the major axes of the inhomogeneity which are defined by two unit vectors lying in a plane parallel to the earth's surface, one of which is parallel with and one of which is normal to the plane of the vertical contact.

The advantage of seeking an admittance tensor rather than a scalar admittance now becomes apparent. Whereas the scalar admittance allows interpretations only in terms of homogeneous layered models, the tensor admittance permits the inclusion of inhomogeneities and anisotropies.

To illustrate the ambiguities arising in the interpretation of a scalar admittance computed for an anisotropic earth consider the following example. A plane wave, elliptically polarized, is assumed to be normally incident on a semi-infinite earth. The eccentricity of the polarization ellipse is taken to be four. The earth consists of a conducting medium which is homogeneous but anisotropic. The major axes of the anisotropy in the horizontal plane are defined by the orthogonal unit vectors $\bar{a}_1$ and $\bar{a}_2$. It is assumed that the component electric and magnetic fields are measured along the axes defined by the orthogonal unit vectors $\bar{u}_1$ and $\bar{u}_2$ oriented at some arbitrary angle θ with respect to the vectors $\bar{a}_1$ and $\bar{a}_2$. Positive values of θ denote clockwise rotations. Along the principal axes and at some frequency, the admittance tensor for the model is assumed to be

$$[Y_{ij}] = \begin{bmatrix} 0 & 1.4e^{-i\pi/4} \\ 2.8e^{-i\pi/4} & 0 \end{bmatrix}.$$

The magnitude of the scalar admittance computed from the component fields obtained for various θ is shown in Fig. 1. The parameter α is the angle between the major axis of the polarization ellipse and the vector $\bar{a}_1$. It may be seen that the scalar admittance is not unique, and, except for the angles $\theta = 0°$ and $\theta = 90°$, shows significant variations with the parameter α. It may be deduced from Fig. 1 that in the case of the real earth possessing local anisotropies and where the electric and magnetic fields are, in general, randomly polarized, it would be difficult indeed to select a scalar admittance for each frequency which would yield meaningful interpretations.

Returning to the problem of determining the admittance tensor elements, it may be seen that if the values of $E_j(\theta)$ and $H_i(\theta)$ are known, then (4) represents two independent equations in the three quantities $Y_{12}(\theta_0)$, $Y_{21}(\theta_0)$ and θ_0. One may obtain known values for $E_j(\theta)$

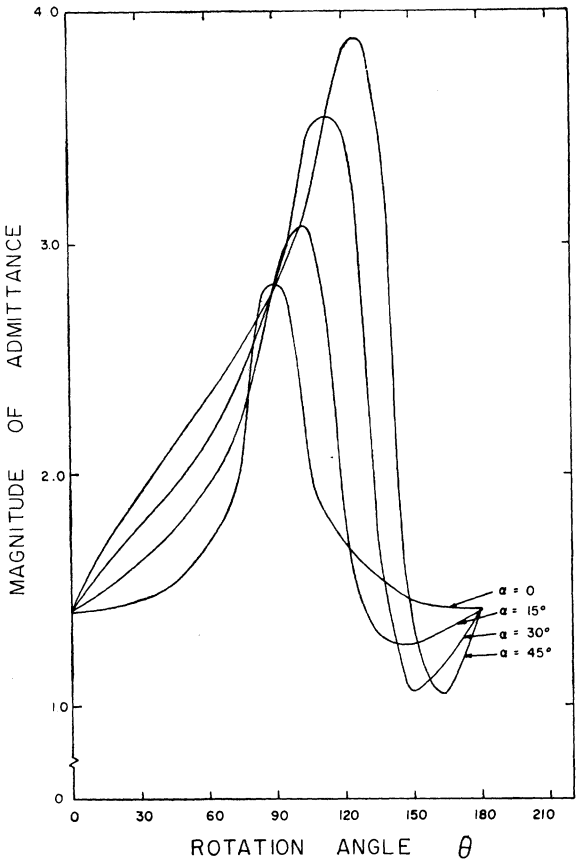

Fig. 1—Scalar admittance solutions as a function of rotation angle for various orientations of a plane elliptically polarized electric field.

and $H_i(\theta)$ from recordings of the tangential electric and magnetic fields obtained at the earth's surface. Since (4) represents but two independent equations in three unknown quantitites, two sets of independent E_j and H_i values are required in order to obtain solutions for the orientation angle θ_0 and the admittance tensor elements along these principal axes.

A straightforward approach would be to write two equations of the form of (4) using the experimental E_j and H_i values and then proceed with an algebraic solution of the resulting equations. Since two independent sets of (4) constitute four independent equations, and there are only three unknown quantities, any three of the four equations would yield a solution. If two sets of solutions were obtained from the four equations by grouping the equations into two different groups of three, and the resulting two sets of solutions were not equal, then one would conclude that the data were not compatible with the assumptions leading to (3). Unfortunately this latter case seems to be the rule rather than the exception. It is easy to show that a nonuniform distribution of sources for the electromagnetic waves or complex shapes for the conductive structures of the earth can cause the computed admittance tensor to possess four independent elements which may not be unique from data sample to data sample.

It has been found, however, that approximate solu-

tions yielding tolerably stable results for most data samples can be found quite simply. The procedure used in this paper is to write (2) with the E_i and H_j values obtained from two independent data samples. The E_i values are obtained from recordings of mutually orthogonal earth current lines and the H_i values are computed from a pair of directional magnetic sensors whose measuring axes are aligned with the earth currents lines. The recording sensors have a fixed angular orientation which, for convenience, is assumed to be defined by the reference unit vectors $\bar{a}_1$ and $\bar{a}_2$, implying that $\theta=0$. The readings of these sensing elements may, however, be transformed to any virtual orientation by applying the appropriate linear transformation.

$$E_j(\theta) = \beta_{jk}E_k(0)$$
$$H_i(\theta) = \beta_{ik}H_k(0), \qquad i, j, k = 1, 2$$

where, for θ clockwise,

$$[\beta_{ik}] = \begin{bmatrix} \cos\theta & \sin\theta \\ -\sin\theta & \cos\theta \end{bmatrix}.$$

Eq. (2) written for the two independent data sets becomes

$$H_i^{\mathrm{I}}(\theta) = Y_{ij}^{\mathrm{I}}(\theta)E_j(\theta)$$
$$H_i^{\mathrm{II}}(\theta) = Y_{ij}^{\mathrm{II}}(\theta)E_j(\theta), \tag{5}$$

where $^{\mathrm{I}}$ and $^{\mathrm{II}}$ denote the two different data samples. Solutions for the four-tensor admittance elements may now be obtained as a function of the virtual orientation angle θ. The values for the admittance elements are in general complex and are not zero for any θ. In many cases, however, the presence of a large-scale inhomogeneity or an extensive anisotropic region which dominates the features of the conductive structures in the vicinity of the measuring site will result in a decided minimum in the magnitude of $Y_{11}(\theta)$ and $Y_{22}(\theta)$ for some $\theta=\theta_0$. Actually four values of θ usually produce minimum values for $|Y_{11}(\theta)|$ and $|Y_{22}(\theta)|$. These are separated by approximately 90° and represent the four orientations for which a pair of orthogonal lines may be aligned with the major axes of the inhomogeneity or the anisotropy. It is usually convenient to restrict θ to the interval $-90°<\theta<90°$, for this is sufficient to define the axes. In order to find the minimum values for $|Y_{11}(\theta)|$ and $|Y_{22}(\theta)|$, these functions may be plotted vs θ, and the minimum values picked visually. It is really necessary to plot only one function, either $|Y_{11}(\theta)|$ and $|Y_{22}(\theta)|$ since in all cases

$$Y_{22}(\theta) = Y_{11}(\theta + 90°).$$

Even though $|Y_{11}(\theta)|$ and $|Y_{21}(\theta)|$ are never actually zero, it is convenient to call the axes along which they are a minimum the principal axes of the admittance tensor.

The values of $Y_{12}(\theta)$ and $Y_{21}(\theta)$ along the principal axes of the admittance tensor may now be obtained as the values of these admittances computed for the angles at which $|Y_{11}(\theta)|$ and $|Y_{22}(\theta)|$ are a minimum. If the magnitude of the phasor angles of the complex admittance elements $Y_{12}(\theta)$ and $Y_{21}(\theta)$ are restricted to values less than 90° and

$$\bar{u}_1 \times \bar{u}_2 = \bar{a}_1 \times \bar{a}_2 = \bar{u}_3,$$

where $\bar{u}_3$ is a vector pointing downward into the earth, $Y_{12}(\theta)$ will generally be negative.

Practically speaking it is usually more convenient to generate and solve (5) if the equations are written in terms of the smoothed power density and cross spectra of the $e_j(t)$ and $h_i(t)$ recordings. The advantages of this operation are two-fold. The computational procedures involved in obtaining the spectral components are usually much shorter for a smoothed power density or cross spectrum than for a detailed Fourier transform. Secondly, the increased bandwidth affords some reduction of the effects of incoherent noise appearing in the data samples. For this reason (5) is rewritten here as

$$\begin{aligned} \Phi_{h_1h_1}(\theta) &= Y_{11}(\theta)\Phi_{h_1e_1}(\theta) + Y_{12}(\theta)\Phi_{h_1e_2}(\theta) \\ \Phi_{h_2h_2}(\theta) &= Y_{21}(\theta)\Phi_{h_2e_1}(\theta) + Y_{22}(\theta)\Phi_{h_2e_2}(\theta) \end{aligned} \tag{6}$$

where Φ_{xx} is the power density spectrum of the signal $x(t)$ and Φ_{xy} is the cross spectrum of the signals $x(t)$ and $y(t)$. One set of (6) may be written using $^{\mathrm{I}}$ and another set using $^{\mathrm{II}}$. Here, as before, these superscripts denote from which of two data samples the spectra are obtained. The procedure for obtaining the admittance tensor elements from (6) is identical with that described above in connection with the solution of (5).

Experimental Results

The details of the instrumentation and recording system at the Electrical Engineering Research Laboratory of the University of Texas have been published previously,[8,9] and will not be repeated here. Over the past year, a large volume of experimental data has been accumulated, but the detailed analysis required in the proposed tensor admittance method has been limited to data taken on four different days. The data selected consists of recordings of approximately 20-minute duration taken during the midmorning hours of August 29, August 30, September 1 and September 5, 1961. The data chosen can generally be classified as typical of "quiet-day" signals. A bandwidth from 0.005 to 1.0 cps was used for all recordings.

[8] R. R. Boothe, B. M. Fannin, and F. X. Bostick, "A Geomagnetic Micropulsation Measuring System Utilizing Air-Core Coils as Detectors," Elec. Engrg. Res. Lab., University of Texas, Austin, Rept. No. 115; August, 1960.

[9] H. W. Smith, L. D. Provazek, and F. X. Bostick, "Directional properties and phase relations of the magnetotelluric fields of Austin, Texas," *J. Geophys. Res.*, vol. 66, pp. 879–888; March, 1961.

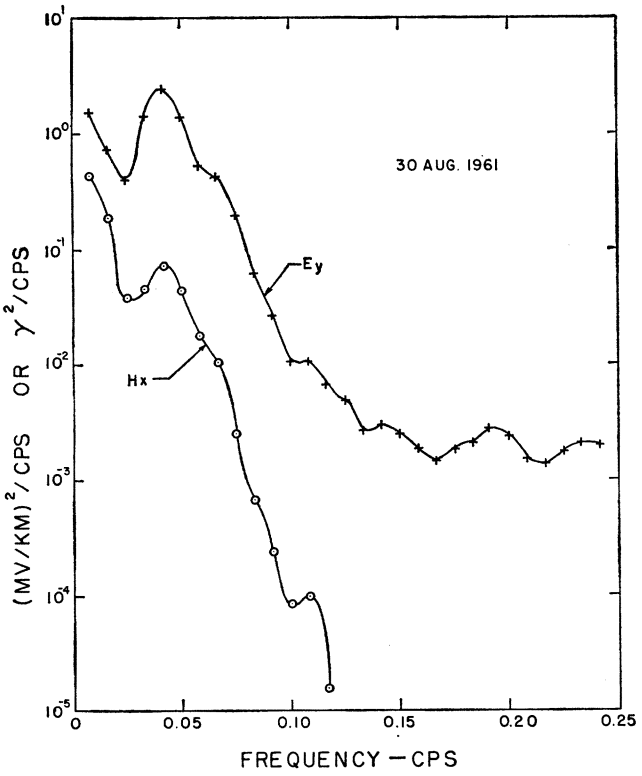

Fig. 2—Power density spectra of H_x and E_y components on August 30.

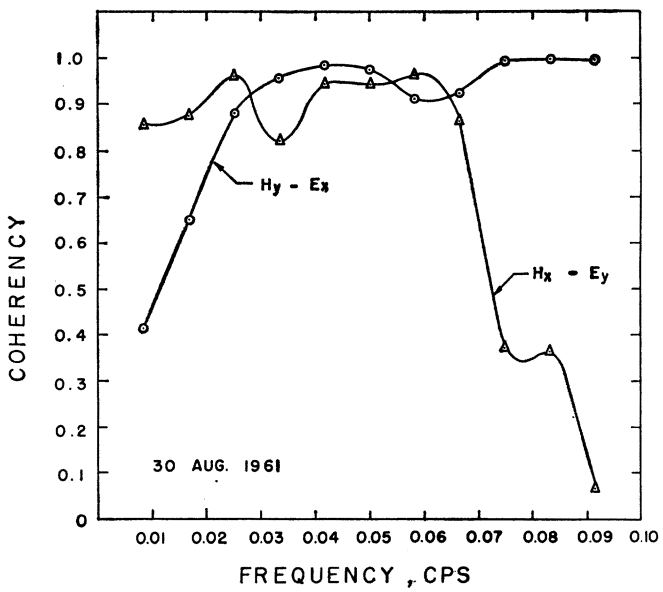

Fig. 3—Coherency plot of H_x-E_y and H_y-E_x combinations on August 30.

The data samples were digitized and all analyses were performed on the CDC-1604 at the University of Texas Computation Center. Statistical procedures recommended by Blackman and Tukey[10] were used throughout in the spectral analysis. The power density spectrum estimates shown in Fig. 2 for the E_x (North-South earth current) and H_y (East-West magnetic field) signals on August 30 are typical for all days. The sharp decrease in the amplitude of these spectra with increasing frequency is characteristic of the data and effectively limits the useful frequency range in the analysis to something below 0.1 cps even though the recording bandwidth is much wider. Prewhitening or filtering techniques are evidently required to increase the usable frequency range to 1 cps or higher because of the limited dynamic range of the recording system.

One of the more significant statistical parameters with respect to the applicability of a particular set of data to this type analysis is the estimate of coherency between the orthogonal electric and magnetic signal components. The coherency between two signals x and y is expressed as

$$\mathrm{coh}_{xy}(\omega) = |\Phi_{xy}(\omega)| / \sqrt{\Phi_{xx}(\omega)\Phi_{yy}(\omega)}, \qquad (7)$$

where $|\Phi_{xy}(\omega)|$ is the magnitude of the cross power density spectra and $\Phi_{xx}(\omega)$ and $\Phi_{yy}(\omega)$ are the individual power densities. Identical signals in a given frequency band would have a coherence of unity. A coherency analysis was made between the two sets of orthogonal signal components for each of the four selected days.

A typical coherency plot is showin in Fig. 3 for the E_x-H_y and E_y-H_x combinations on August 30, 1961. The sharp decrease in coherency between the H_x-E_y signals for frequencies above about 0.07 cps is characteristic of the data on all of the four days. An attempt to extend the analysis into the frequency range of low coherency signals resulted in erratic and inconsistent results as contrasted with those obtained using high coherency signals. It would thus appear that highly coherent orthogonal signal components are essential to this type of analysis. For this reason the results in this paper are restricted to a very limited frequency range.

The resistivity values determined from both the E_x-H_y and E_y-H_x signal combinations for all four days were computed as in (1) except that the ratio of power density spectra were used to add bandwidth to the process. The bandwidth chosen was 0.00833 cps. The results of this analysis are shown in Fig. 4. Points designated $\rho_{21}(0°)$ and $\rho_{12}(0°)$ represent, respectively, the "Cagniard" resistivities obtained on August 29 using the E_x-H_y and E_y-H_x signal pairs for measuring axes aligned at zero degrees or in North-South, East-West directions. Points designated $\rho_{21}(-45°)$ and $\rho_{12}(-45°)$ are corresponding values for measuring axes which have been rotated 45° in a counterclockwise direction. The rotation of the measuring axes was accomplished by appropriate transformations on the computer rather than a physical realignment of the system. The total spread of values indicated on Fig. 4 represent the extremes of resistivity obtained for all four days for rotation angles from 0° to 90° in 15° increments. The total number of resistivity computations represented in the

[10] R. B. Blackman and J. W. Tukey, "The Measurement of Power Spectra," Dover Publications, Inc., New York, N. Y.; 1958.

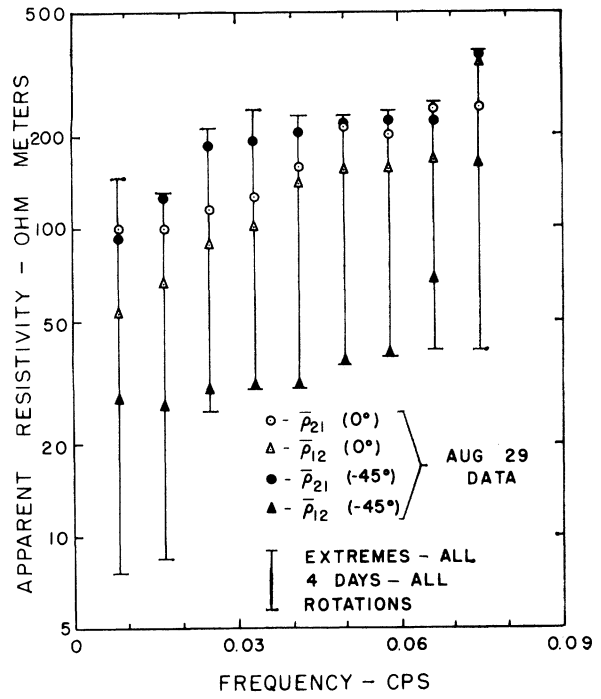

Fig. 4—Apparent resistivity values computed from (1).

figure is 432. The total spread in resistivity values is seen to be quite large even though signals with a high coherency were used throughout. It would appear meaningless to attempt to fit these results to Cagniard's two-layer curves.

Fig. 5 shows the results obtained from the computation of $|Y_{21}|$ and $|Y_{11}|$ as a function of the rotation angle, θ, for four selected frequency bands using the data for August 30 and September 1. Curves for $|Y_{12}|$ and $|Y_{22}|$ were not plotted since, as pointed out above, the model requires that $|Y_{22}(\theta)| = |Y_{11}(\theta+90°)|$ and $|Y_{12}(\theta)| = |Y_{21}(\theta+90°)|$. Hence, for any value of θ in Fig. 5, $|Y_{12}|$ and $|Y_{22}|$ are found at an abscissa of $\theta+90°$. Similar computations were made for each of nine frequency bands for all possible pairs of data taken on different days. Thus six sets of curves of the type shown in Fig. 5 were obtained. Of course, only two sets represent completely independent data, but the two independent sets could be taken in three different combinations. All six were computed and plotted to show the total spread of values obtained.

One of the most significant features of the curves in Fig. 5 is the double null in $|Y_{11}|$; the nulls in each case are approximately 90° apart. Out of a total of 54 sets of these curves for the different frequency bands, only four did not show this characteristic. In accordance with the theory the best estimate of the magnitude of the admittance along the major axes of the anisotropy, are the values on the $|Y_{21}(\theta)|$ curve corresponding to the nulls of the $|Y_{11}(\theta)|$ curve. These values are designated $|Y_{21}(\theta_0)|$ and $|Y_{12}(\theta_0)|$ where θ_0 is the rotation angle corresponding to the null.

The rotation angles, θ_0, required for the double null condition of $|Y_{11}|$ and $|Y_{22}|$ are plotted in Fig. 6 as a function of frequency for each set of data. The total spread of null rotation angles is from −30° to −60° with an average somewhere near −45°. Since 15° increments were used in the rotation analysis, the fluctuations with frequency in Fig. 6 probably have little significance except that they lie within a total spread of approximately 30°.

From the values of $|Y_{21}(\theta_0)|$ and $|Y_{12}(\theta_0)|$ obtained from curves of the type shown in Fig 5, the values of resistivity along the principal axes were computed from the relation

$$|Y| = \frac{1}{\sqrt{i\omega\mu\rho}}.$$

The average value and the extremes of $\rho_{21}(\theta_0)$ and $\rho_{12}(\theta_0)$ for all six sets of data are shown in Fig. 7 as a function of frequency. With the exception of the 4 points discarded for lack of double nulls in the $|Y_{11}|$ curves, the extremes and averages for each frequency band are based on six computed resistivity values.

Conclusions

There are several features of Fig. 7 which appear to be significant. The distinct separation between the ρ_{21} and ρ_{12} resistivities at all frequencies suggests a large-scale anisotropy or inhomogeneity in the earth, with a major axis along a line approximately 45° in a counterclockwise direction from true North. Higher resistivity values are found along this major axis and appreciably lower values are found along the minor axis. The total spread of values for both ρ_{21} and ρ_{12} is considerably reduced over the corresponding results in Fig. 3, and are almost completely contained within the extremes of that plot.

Looking only at very gross geological features of the region within 100 miles of the measuring site in Austin, they may be described in terms of sedimentary deposits of relatively low resistivity in nearly all directions with the exception of a large granite outcrop called the Llano uplift approximately 50 miles to the Northwest. The map shown in Fig. 8 indicates the location of the measuring site relative to this large outcrop of pre-Cambrian rock. It is tempting to attribute the observed results to this abrupt geological anomaly, but it is hardly warranted on the basis of present knowledge of either the geology or the model. It is encouraging, however, that the results consistently show the major axis of the anisotropy and the higher resistivity value in the direction of this known anomaly.

In conclusion it appears that even though the exactly solvable cases are fundamentally too simple to expect in reality, the tensor admittance method can significantly increase the utility of the magnetotelluric analysis. Subjective interpretations of the analyzed data can be quite meaningful since at least one of the principal ambiguities in the analysis methods has been eliminated.

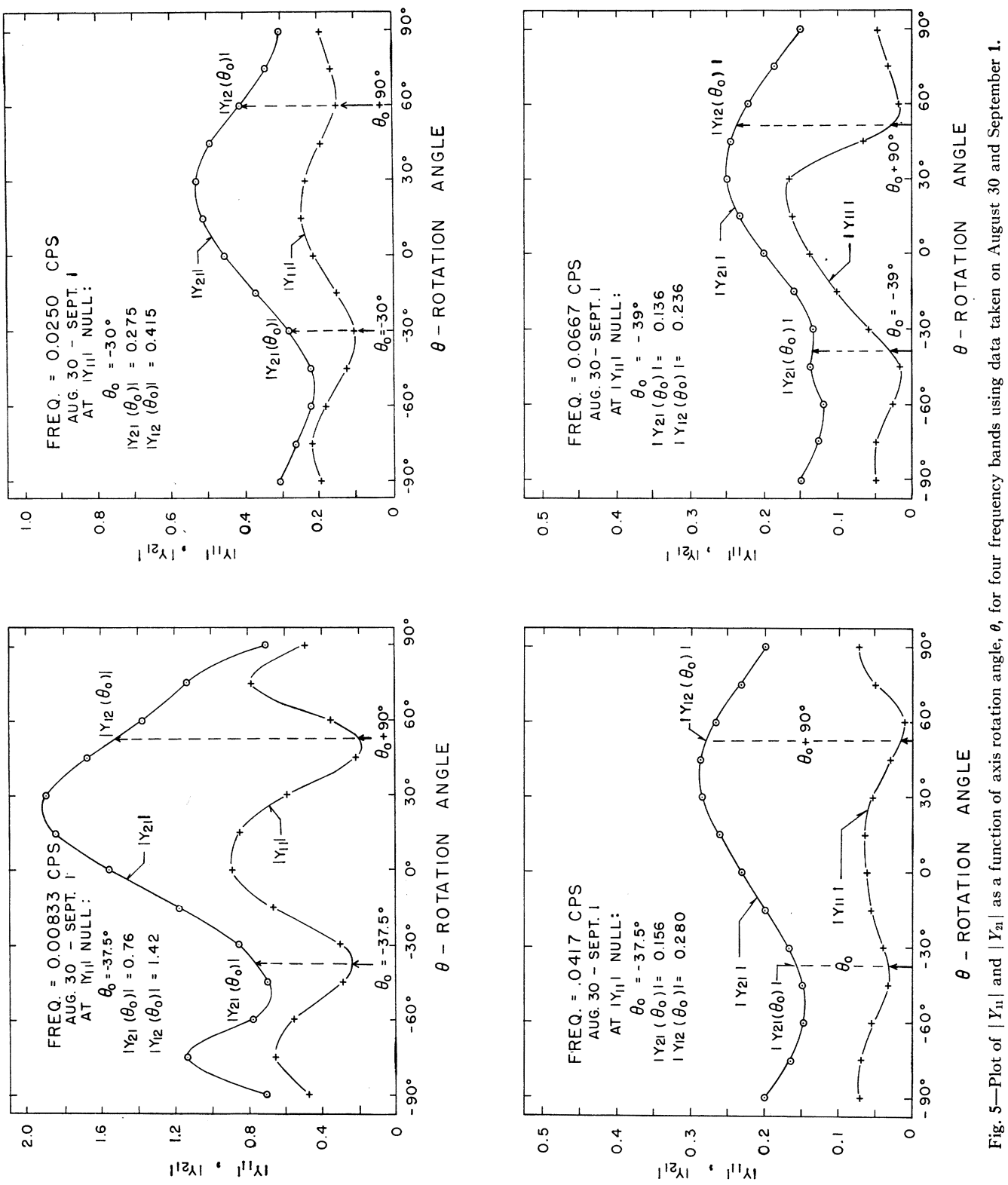

Fig. 5—Plot of $|Y_{11}|$ and $|Y_{21}|$ as a function of axis rotation angle, θ, for four frequency bands using data taken on August 30 and September 1.

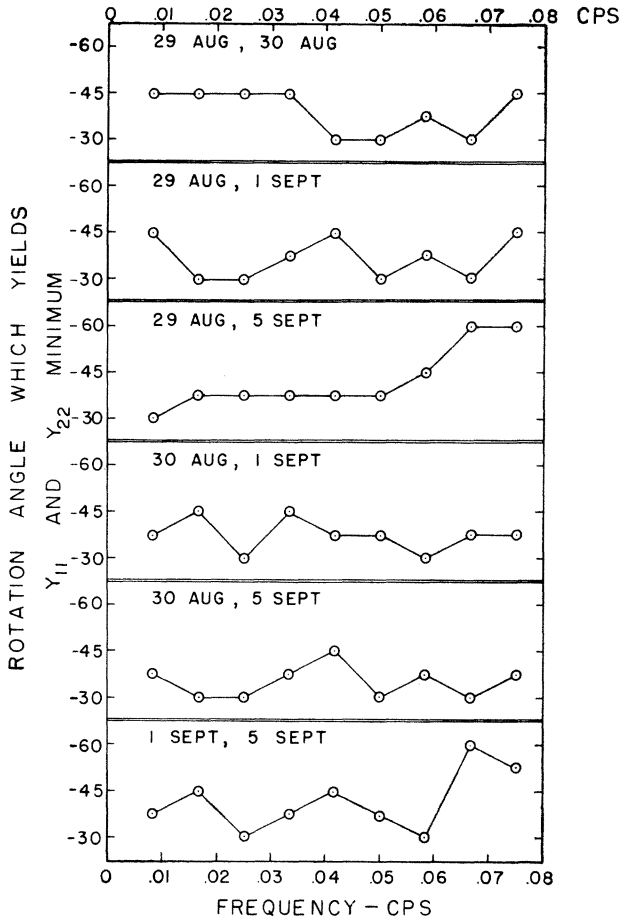

Fig. 6—Plot of rotation angle, θ_0, which yields minimum values of $|Y_{11}|$ and $|Y_{22}|$.

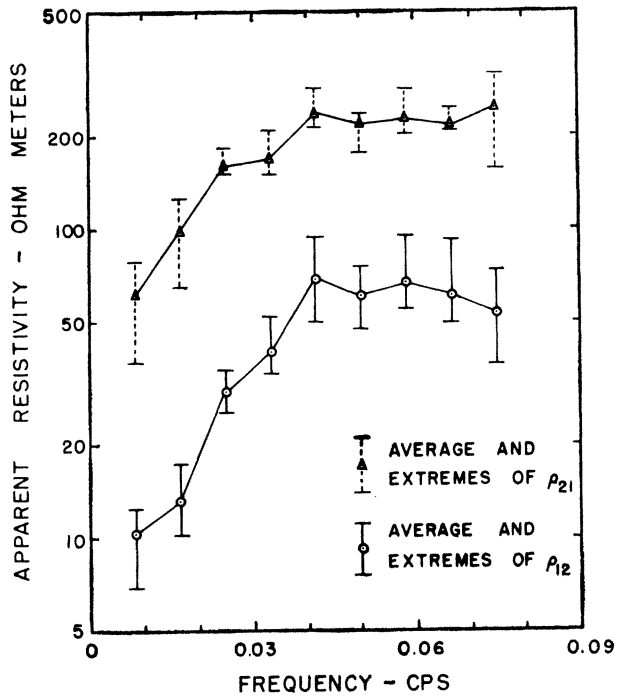

Fig. 7—Apparent resistivity values along major and minor axis for rotation angle θ_0.

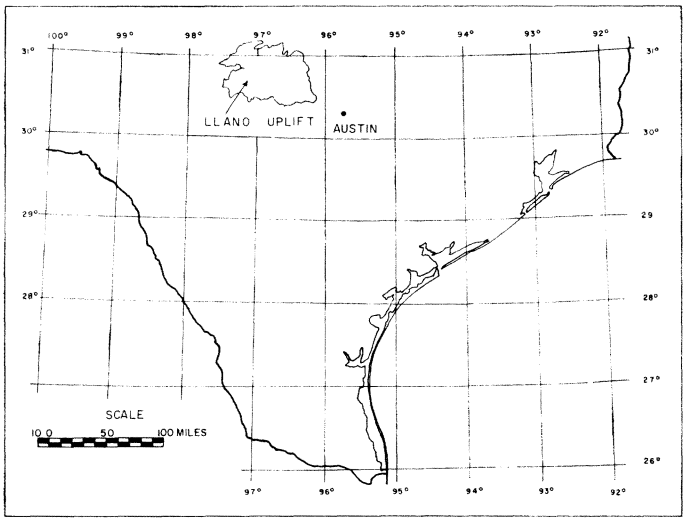

Fig. 8—Map of Texas showing the location of Austin relative to the large granite outcrop in the Llano uplift region.